Development 139, 2187-2197 (2012) doi:10.1242/dev.073734
© 2012. Published by The Company of Biologists Ltd

Cytoskeletal changes in actin and microtubules underlie the developing surface mechanical properties of sensory and supporting cells in the mouse cochlea

Katherine B. Szarama[1,2,3,‡], Núria Gavara[1,*], Ronald S. Petralia[4], Matthew W. Kelley[2] and Richard S. Chadwick[1]

SUMMARY

Correct patterning of the inner ear sensory epithelium is essential for the conversion of sound waves into auditory stimuli. Although much is known about the impact of the developing cytoskeleton on cellular growth and cell shape, considerably less is known about the role of cytoskeletal structures on cell surface mechanical properties. In this study, atomic force microscopy (AFM) was combined with fluorescence imaging to show that developing inner ear hair cells and supporting cells have different cell surface mechanical properties with different developmental time courses. We also explored the cytoskeletal organization of developing sensory and non-sensory cells, and used pharmacological modulation of cytoskeletal elements to show that the developmental increase of hair cell stiffness is a direct result of actin filaments, whereas the development of supporting cell surface mechanical properties depends on the extent of microtubule acetylation. Finally, this study found that the fibroblast growth factor signaling pathway is necessary for the developmental time course of cell surface mechanical properties, in part owing to the effects on microtubule structure.

KEY WORDS: Young's modulus, Fgf signaling, Organ of Corti, Mouse

INTRODUCTION

Cells and tissues withstand mechanical stress during differentiation and development. One key mediator of mechanical stress is the formation of the cytoskeleton, which dictates both the cellular response to external force and cellular force transmission (Janmey, 1998; Mammoto and Ingber, 2010). Both internal genetic and external biochemical cues can influence not only developing cell structure but also cell mechanical properties. Disruptions to these signaling pathways in developing and developed tissues also disturb cell mechanical properties, ultimately impairing organ function (Safar et al., 2004; Lane and Yao, 2010). Therefore, the regulation of the cytoskeleton and the impact of that regulation on cell mechanics are important questions for development.

The mammalian inner ear is an excellent model system for investigating basic cell biology questions about the mechanical cues that guide cell shape and mechanical properties. The organ of Corti develops both specialized sensory hair cells that detect and amplify sound vibrations, and non-sensory supporting cells that withstand the mechanical deformations of sound transmission (Anniko, 1983). At the cellular level, mechanosensory outer hair cells (OHCs) are primarily composed of actin filaments (Anniko, 1983; Raphael et al., 1994; Etournay et al., 2010) that vary by isotype and by partnership with motors and binding proteins (Slepecky and Chamberlain, 1985; Self et al., 1999; Furness et al., 2005). In contrast to OHCs are non-sensory supporting cells, such as pillar cells (PCs), which contain a remarkable density of microtubules that are thought to provide structural and functional support in the fluid flow of the traveling sound wave through the organ of Corti (Tolomeo and Holley, 1997; Hallworth et al., 2000; Karavitaki and Mountain, 2007). Previous work has focused on the role of the cytoskeleton in dictating the shape and polarity of these cells in the cochlea, particularly in the context of cell specification and orientation within the sensory epithelium (Fritzsch et al., 2002; Kelley, 2007; Kelly and Chen, 2007). However, the molecular mediators organizing the development of the cytoskeleton and dictating the mechanical properties of the cochlea have not been addressed.

One potential mediator of cell structural development is the fibroblast growth factor (Fgf) family of receptors. These tyrosine kinase receptors are spatially regulated by the presence of Fgf ligands and proteoglycans (Ornitz, 2000), and temporally regulated throughout development (Jacques et al., 2007). This pathway has been implicated specifically in supporting PC development, as mutations in the gene encoding Fgf receptor 3 (*Fgfr3*) lead to collapsed PCs and hearing impairment (Colvin et al., 1996; Hayashi et al., 2007; Puligilla et al., 2007). Furthermore, upregulation of Fgf signaling delays the differentiation of PCs (Jacques et al., 2007). These studies suggest that proper growth factor signaling might regulate cytoskeletal formation and could dictate the developmental time course of cell mechanical properties.

Measuring cell surface mechanical properties can be accomplished quantitatively by calculating the Young's modulus of a cell using an atomic force microscope (Fig. 1). Young's modulus, also referred to as stiffness, is a material property describing the resistance of structure to mechanical deformation, where an increasing Young's modulus indicates cell stiffening

---

[1]Section on Auditory Mechanics, Laboratory of Cellular Biology, National Institute on Deafness and other Communication Disorders, National Institutes of Health, Bethesda, MD 20892, USA. [2]Section on Developmental Neuroscience, Laboratory of Cochlear Development, National Institute on Deafness and other Communication Disorders, National Institutes of Health, Bethesda, MD 20892, USA. [3]Center for Hearing and Communication Research, Department of Clinical Science, Intervention, and Technology, Karolinska Institutet, Stockholm, Sweden. [4]Advanced Imaging Core, National Institute on Deafness and other Communication Disorders, National Institutes of Health, Bethesda, MD 20892, USA.

*Present address: Drittes Physikaliches Institut, Georg-August-Universität, Göttingen, Germany
‡Author for correspondence (szaramak@nidcd.nih.gov)

Accepted 5 April 2012

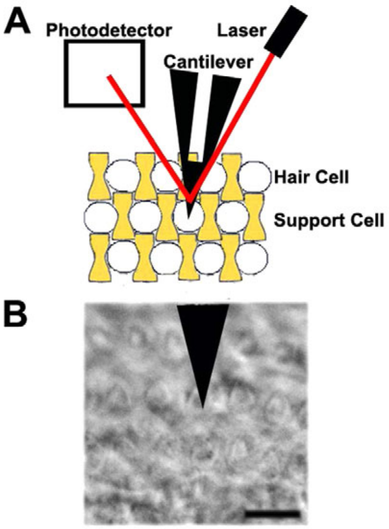

Fig. 1. Atomic force microscope (AFM) setup to measure cell surface mechanical properties of the inner ear. (**A**) In this AFM setup, a cantilever probes sensory hair cells (white) or non-sensory support cells (yellow) by measuring deflection of the laser (red) reflected off the surface of the cantilever and onto a photodetector. (**B**) Phase-contrast image of outer hair cell in contact with AFM cantilever. Scale bar: 10 µm.

(Murakoshi et al., 2006). As the structural organization of cells in the cochlea is specific to transmit mechanical sound stimuli, the measurement of the cell stiffness can lead to further understanding the important developmental events within the inner ear. For example, structural maturation of the organ of Corti during postnatal development includes the formation of the inner sulcus, the release of the tectorial membrane, the formation of the spaces of Nuel and the opening of the tunnel of Corti, which coincides with the onset of hearing function (Pujol and Hilding, 1973). Therefore, elucidating the mechanical properties of this sensory epithelium at a cellular level has implications for quantitatively describing changes in tissue architecture and further understanding hearing function.

Here, we show the interplay between developing cytoskeletal structures and maturing cell surface mechanical properties. We find that maturing OHC surface mechanical properties primarily depend on actin, but that microtubules are required early in OHC structural and mechanical development. By contrast, supporting PC surface mechanical properties are only dependent on microtubules at later developmental time points. Finally, our results suggest a potential role for the Fgf signaling pathway in regulating both the timing of developing cell mechanical properties in the organ of Corti and the changing dynamics of the actin cytoskeleton.

MATERIALS AND METHODS

Cochlear explant cultures and pharmacological treatments

All experiments were performed on Institute for Cancer Research mice. All animal care and procedures were approved by the Animal Care and Use Committee at NIH and complied with NIH guidelines for the care and use of animals. Cochleae were dissected to expose the lumenal surface of the cochlear duct and cultured to the desired age as previously described (Montcouquiol and Kelley, 2003) but plated on No.1 glass cover slips (Corning). Tissue cultures were treated after 12-17 hours in vitro for 30 minutes with one of the following: 1 µM latrunculin A, 5 µM jasplakinolide, 10 µM blebbistatin, 1 µM taxol (Sigma) in DMSO, 5 µM nocodazole (Sigma) in PBS, or vehicle control added to Leibovitz's medium (GIBCO, Invitrogen). To affect the Fgf signaling pathway, tissue explants were treated immediately after plating with either 10 µM SU5402 (EMD Chemicals) in DMSO, or 1 µM Fgf2 (R&D Systems) in PBS with 0.1% DMSO and 1 µg/ml heparin alone or in combination with one of the following: 5 µM Y27632 (Sigma) in sterile water, 10 µM SP600125 (Sigma), or 1 µM U0126 (Sigma) in DMSO.

Transmission electron microscopy

Cochleae from three mice at each age were isolated and placed immediately in 4% paraformaldehyde with 2% glutaraldehyde containing 0.1 M phosphate buffer (pH 7.4) for 30 minutes at room temperature then 2 hours at 4°C. The inner ears were washed in phosphate buffer and then 0.1 M cacodylate buffer, post-fixed with 1% osmium tetroxide, dehydrated through a graded alcohol series and stained with 1% uranyl acetate in 50% ethanol. Samples were embedded in Poly/BED 812 resin (Polysciences, Warrington, PA, USA) as previously described (Petralia and Wenthold, 1992). Sections of ~75 nm were cut using a Leica Reichert ultramicrotome, stained with 0.03% lead citrate for 3 minutes and examined using a JEOL transmission electron microscope at 80 kV.

Immunohistochemistry

Samples were fixed in 4% paraformaldehyde and rinsed in PBS. Nine whole-mount cochleae and six cross-sections from six cochleae for each age were examined. Samples shown in cross-section were passed through a 5-30% sucrose gradient and cryosectioned at 12 µm thickness. Samples were permeabilized with 0.2% Tween-20, blocked with 10% normal horse serum and incubated overnight in primary antibody (anti-acetylated tubulin, Sigma, 1:75; anti-p75 neurotrophin receptor, Covance, 1:1000; anti-ZO-1, Millipore, 1:1000; anti-β-tubulin I and II, Sigma, 1:200) at 4°C. Primary antibodies were detected using either Alexa Fluor 488- or 546- (Invitrogen, 1:1000) conjugated secondary antibodies. Directly conjugated Phalloidin 633 (Invitrogen, 1:5000) was applied to all samples. All fluorescence images were acquired using a Zeiss 510 LSM Confocal Microscope using a 20× objective. To measure relative fluorescence intensity, a 20 μm^3 average intensity *z*-projection was reconstructed using ImageJ analysis software (Rasband, 1997). Average gray values (mean±s.e.m. arbitrary units, AU) were calculated from 36 cells repeated for six animals.

Atomic force microscopy and live cell imaging

Experiments were performed using a Bioscope II and Bioscope Catalyst AFM (Bruker) head mounted onto a Zeiss Axiovert 200 inverted microscope and controlled via Nanoscope V controller. Pyramidal shaped, gold-coated, silicon nitride cantilever probes with 0.03 N/m nominal spring constant (Bruker) were used for all measurements. Cells were identified after being loaded with 500 nM Calcein AM vital dye (Invitrogen) in Leibovitz's medium for 30 minutes and rinsed with fresh Leibovitz's medium. Measurements were performed in 'contact mode' in Leibovitz's medium as previously described (Gavara and Chadwick, 2010) with 1.5 µm indentation to construct three force-distance curves at the center of each identified cell. For line-scan measurements, a 50 μm^2 region of interest was selected and points over the lumenal surface of the second row of outer hair cells and pillar cell rows were examined with 2 µm equal spacing. Because the base of inner hair cells are rotated in explant cultures, these measurements were excluded from the analysis. Relative force-distance curves were collected with ~300 nm trigger threshold using 3 µm force ramping at 1 Hz for three cycles. Data were analyzed with custom analysis software in MATLAB to fit force-distance curves to the Sneddon cone model (Sneddon, 1965) and to calculate the Young's modulus using the formula $F=(2/\pi\tan\alpha)(E/(1-\nu^2))\delta^2$; where F is applied force, ν is Poisson's ratio (assumed to be 0.5), δ is cantilever indentation and α is cantilever tip angle. Average Young's modulus (mean±s.e.m. kPa) was calculated from the average measurements of ten cells for seven to ten animals within a basal or apical region of the cochlea. Statistical analyses were performed using Shapiro-Wilk normality test, Kolmolgorov-Smirnov distribution difference test and Welch's *t*-test. All *P*-values were corrected with the Bonferroni correction for multiple testing.

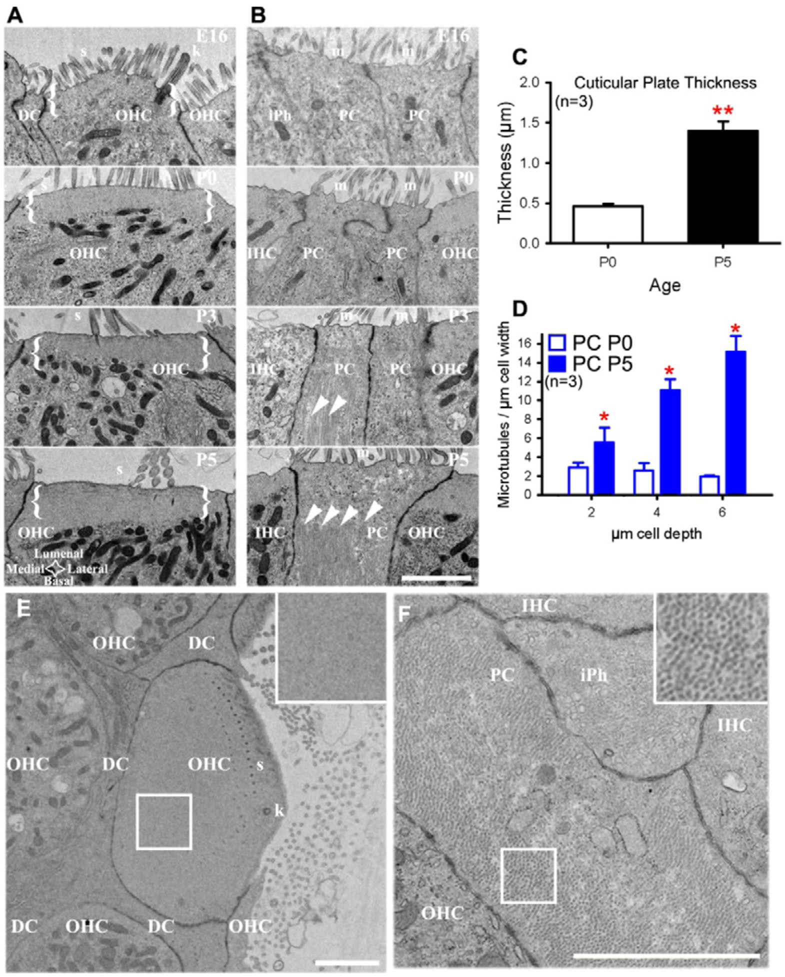

Fig. 2. Outer hair cells and pillar cells have different cytoskeletal arrangements. (**A**,**B**) Representative transmission electron micrographs of cochlear cross-sections reveal changes in cuticular plate thickness (A, brackets) in outer hair cells (OHCs) from E16 to P5, and more microtubules (B, arrowheads) in supporting pillar cells (PCs). (**C**,**D**) Quantification shows significant increase in cuticular plate thickness of OHCs (C, $**P<0.001$) and more microtubules in PCs (D, $*P<0.05$) from P0 to P5. Error bars represent s.e.m. (**E**,**F**) Horizontal sections of P3 OHC (E) and PC (F) with insets (box) showing homogeneous distribution of actin in the cuticular plate of OHC and anisotropic microtubules in PC. Scale bars: 2 µm. DC, Deiter's cell; IHC, inner hair cell; iPh, inner phalangeal cell; s, stereocilia; k, kinocilium; m, microvilli.

RESULTS

Outer hair cells and supporting pillar cells have different cytoskeletal components

To identify which cytoskeletal components might affect mechanical properties of OHCs and PCs, we performed transmission electron microscopy on cochlear cross-sections. OHCs had an actin-rich cuticular plate that was evident at postnatal day (P)0 and increased in thickness up to P5 (Fig. 2A, brackets). By contrast, PCs had very little obvious cytoskeletal structure at embryonic day (E)16 and P0 (Fig. 2B). Later, at P3 and P5, PCs had anisotropic microtubules that ran parallel to the cell's main axis (Fig. 2B, arrowheads). To quantify the structural development of OHCs, we analyzed cuticular plate thickness at P0 and P5 (Fig. 2C) and found a 66% increase in thickness between these time points ($P<0.001$). We also counted the number of microtubules in PCs and found significantly more microtubules at P5 relative to P0 (Fig. 2D; $P<0.05$). To understand the distributions of actin and microtubules in OHCs and PCs, we examined electron micrographs of horizontal sections from P3 cochleae. The OHC cuticular plate had a homogeneous distribution of actin (Fig. 2E, inset) at the lumenal surface. By contrast, PCs contained anisotropic microtubules throughout the cell cytoplasm oriented from apical to basal poles of the cell (Fig. 2F, inset). Overall, these specialized cytoskeletal distributions were seen within the first postnatal week of development, and are consistent with the well documented differences in these cell types at mature stages (Raphael et al., 1994; Nishida et al., 1998; Furness et al., 2005). Because these cell types have established mechanical differences at adult stages (Tolomeo et al., 1996; Naidu and Mountain, 1998; Scherer and Gummer, 2004), we wanted to ascertain when these differences in mechanical properties arise during development.

Outer hair cells have different surface mechanical properties than supporting pillar cells

To determine the development of OHC and PC surface mechanical properties, we applied atomic force microscopy (AFM) to cochlear explant cultures and acquired force-distance measurements of OHCs and PCs at the lumenal cell surface. We calculated and compared the Young's modulus, which is a material property of stiffness, for OHCs and PCs in the base and apex of the cochlea at specific time points between E16 and P5 (Fig. 3). In the base of the cochlea, the OHC stiffness had a peak distribution that did not overlap with PC stiffness at all postnatal time points (Fig. 3A-D) and had a significantly different distribution from PC stiffness at E16, P0 and P3 ($P<0.05$). Overall, PCs were softer than OHCs from E16 to P3 and had a distribution that was skewed left at all measured time points (Fig. 3A-D). In the cochlear apex, the peak OHC stiffness was distinct from PCs at P0 and P5 (Fig. 3E-H) and these cell types had significantly different distributions in cell surface mechanical properties from P0 to P5 ($P<0.05$). Furthermore, at P0 and P3, the OHC Young's modulus had a normal distribution (Fig. 3E-H, $P<0.05$) whereas the PC distribution was skewed left.

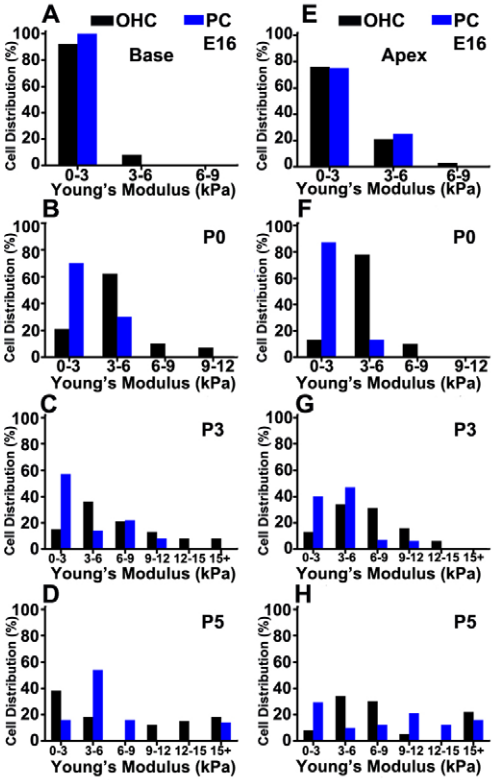

Fig. 3. OHCs and PCs have different mechanical properties. (**A-D**) Histogram plots show different distributions in Young's modulus between basal OHCs (black) and PCs (blue) from E16 to P5 ($P<0.05$). (**E-H**) In apical regions, OHCs and PCs have similar distributions at E16. However, by P0 and P3, OHC Young's modulus has a normal distribution ($P<0.05$) whereas PC Young's modulus distribution is skewed left. Young's modulus (kPa) is binned and plotted as distribution of 70-90 cells measured (%).

The patterning of this sensory epithelium consists of distinct rows of OHCs and PCs that are organized during embryonic development. To examine differences across this epithelium, we measured stiffness along OHC and PC rows, and calculated Young's modulus at equally spaced intervals in the longitudinal direction of the cochlea. OHC rows develop local heterogeneity in stiffness during the postnatal period (Fig. 4). At P0, areas within OHCs (Fig. 4D, shaded) are relatively similar to areas between OHCs (Fig. 4D, unshaded). Calculating the relative height differences along the line scan revealed <1 μm variation in the OHC row (Fig. 4D′). By P3, the areas between OHCs became stiffer than those within individual OHCs (Fig. 4E,F). Looking at the regions that are most stiff at P5, relative height data showed that the regions between OHCs corresponded to local minima (Fig. 4F′) and might represent the stiffness of Deiter's cells (DCs), which interdigitate between OHCs (Fig. 2E). Moreover, the stiffness measurements in line scans of this row became more heterogeneous as development proceeded from P0 to P5 (Fig. 4), which might coincide with the development of DC surface mechanical properties.

In contrast to the OHC row, the PC row showed little heterogeneity at P0, P3 and P5 (Fig. 5D-F). PCs were identified with live cell fluorescence imaging, and relative height data showed that regions within a PC had <0.5 μm variation (Fig. 5D′-F′, shaded). Areas in the PC row that did not contain identifiable PCs (Fig. 5, unshaded) included cell contacts, inner hair cells or inner phalangeal cells, which separate inner hair cells from PCs (Slepecky and Chamberlain, 1985). At P0, regions within PCs (Fig. 5D, shaded) were relatively similar to areas between PCs (Fig. 5D, unshaded). By P3, regions between PCs were stiffer than regions within PCs (Fig. 5E). There was also increased stiffness along the PC row between P3 and P5 (Fig. 5F), but <1 μm variation in relative height (Fig. 5F′). Taken together, atomic force microscope measurements are cell specific and suggest that OHC surface mechanical properties differ from PCs, and that OHC rows have a stiffness heterogeneity that is not found in PC rows.

Increasing outer hair cell and supporting pillar cell stiffness corresponds to the acquisition of actin filaments and acetylated microtubules, respectively

To identify the cytoskeletal mechanisms underlying developing cell mechanics, we first immunolabeled actin filaments and acetylated tubulin in the sensory epithelium. Confocal projections of cochlear cross-sections revealed that phalloidin localized to the lumenal surface of the sensory epithelium (Fig. 6A). Also, the fluorescence intensity of phalloidin increased gradually in OHCs from E16 to P5, suggesting an accumulation of actin in these cells. An antibody raised to acetylated tubulin was used to identify a subset of stable microtubules, as previous studies have shown a high correlation between microtubule stability and acetylation (Bane et al., 2002; Westermann and Weber, 2003). Immunofluorescence was found primarily in PCs and DCs in both the lumenal and basolateral surfaces of the sensory epithelium (Fig. 6A). Also, fluorescence intensity increased dramatically in PCs between P3 and P5.

Next, we compared the average Young's modulus at embryonic and postnatal time points. OHC stiffness gradually increased up to P3, but was not significantly different between P3 (6.71±0.98 kPa) and P5 (7.41±1.02 kPa) (Fig. 6B). Quantifying relative fluorescence intensity between E16 and P5 in OHCs also revealed a 72% increase in phalloidin intensity, but relatively consistent acetylated tubulin (Fig. 6B; $P<0.01$). By contrast, PC surface mechanical properties remained unchanged early in development between E16 (2.58±0.29 kPa) and P3 (3.46±0.61 kPa) (Fig. 6C). Between P3 and P5, PC Young's modulus increased 66%, which was statistically significant (Fig. 6C; $P<0.001$). Quantifying relative fluorescence intensity between E16 and P5 in PCs revealed an 80% increase in acetylated tubulin and a 69% increase in phalloidin (Fig. 6C). Thus, the development of hair cell and pillar cell surface mechanical properties coincides with the developmental acquisition of actin and acetylated microtubules, respectively.

Outer hair cell stiffness requires actin, but pillar cell stiffness does not

The rate of actin accumulation and OHC stiffening suggests that actin dynamics contribute to the developing mechanical properties of OHCs. To test this hypothesis, cochlear cultures were incubated with latrunculin A, which sequesters actin monomers (Coué et al., 1987; Bershadsky et al., 1995) and prevents actin filament polymerization (Ayscough et al., 1997) and should, therefore soften, OHCs. Confocal *z*-projections of latrunculin A-treated cultures showed decreased phalloidin fluorescence intensity and mislocalization of the tight junction protein zonula occludens 1 (ZO-1; Tjp1 – Mouse Genome Informatics) relative to control at P0 and P3 (Fig. 7A,B). Quantifying average fluorescence intensity at P0

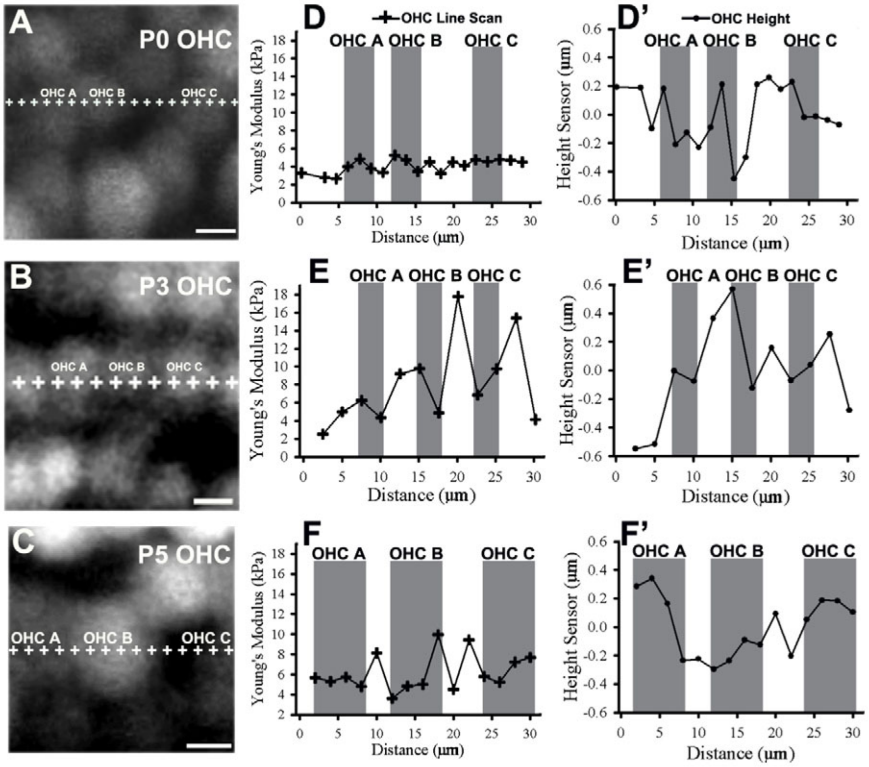

Fig. 4. Outer hair cell rows show heterogeneity in surface mechanical properties. (**A-C**) Fluorescence images of Calcein AM-labeled second row OHCs from P0, P3 and P5 show locations of line scan measurements (+). (**D-F**) Young's modulus (kPa) of OHCs is plotted against 30 µm longitudinal distance and corresponds to images A-C, respectively. Shaded regions correspond to OHCs shown at left. Data show increasing heterogeneity in Young's modulus within OHC rows from P0 to P5. (**D′-F′**) Relative height (µm) differences in second OHC row show little variation in shaded regions along the line scan distance (µm). Scale bars: 5 µm.

revealed significantly decreased F-actin from 538±48 AU in control to 261±35 AU in latrunculin A-treated OHCs (Fig. 7C; *P*<0.01). At P3, latrunculin A significantly decreased average fluorescence intensity of F-actin, with a 69% decrease in the OHCs and a 43% decrease in the PCs (Fig. 7D). The presence of actin filaments primarily in OHCs suggested that a decrease in filaments would decrease OHC stiffness. First, we set out to determine the time course of changing cell surface mechanical properties. Force-distance measurements were collected from OHCs in latrunculin A- and vehicle control-treated cultures at 10 minute intervals following drug delivery. We found that control OHCs showed little change in Young's modulus after 60 minutes of continuous force ramping (supplementary material Fig. S1A), and at discrete stages of both embryonic and postnatal development (supplementary material Fig. S1B). By contrast, OHC Young's modulus decreased in the presence of latrunculin A at E16 and P0 (supplementary material Fig. S1C,D).

To assess population changes in surface mechanical properties, average Young's modulus was compared between latrunculin A cultures and vehicle control. OHCs were significantly softer in treated cultures relative to control at P0 (1.36±0.13 kPa and 4.13±0.26 kPa, respectively) and P3 (2.54±0.61 kPa and 6.94±0.36 kPa, respectively) (Fig. 7C,D; *P*<0.001). However, no significant change in Young's modulus was observed between treated and control PCs (Fig. 7C,D; *P*>0.05), suggesting that actin does not play a significant role in the acquisition of surface mechanical properties of these cells. However, we could not rule out the possibility that the actin cytoskeleton in postnatal PCs (Fig. 6) might contribute to PC surface mechanical properties. To understand further the impact of the actin network on surface mechanical properties of these cells, cochlear cultures were treated with either jasplakinolide, which polymerizes actin filaments (Bubb et al., 1994; Bubb et al., 2000), or blebbistatin, a small molecule specific inhibitor of myosin II activity (Straight et al., 2003; Limouze et al., 2004; Kovacs et al., 2004), to drive reorganization of the actin cytoskeleton (Bridgman et al., 2001; Guha et al., 2005; Murthy and Wadsworth, 2005). Cultures treated with jasplakinolide had significantly stiffer OHCs and PCs at P0 and P3 (Fig. 7E), confirming our previous results that actin polymerization can increase cell stiffness. Cultures treated with blebbistatin had significantly stiffer PCs at P0 (Fig. 7F; 3.95±0.42 kPa; *P*<0.01) and significantly softer PCs at P3 (Fig. 7F; 1.87±0.28 kPa; *P*<0.05), suggesting that myosin II activity can alter the actin cytoskeleton to drive changes in PC surface mechanical properties. Changes in OHC surface mechanical properties were also significantly affected by treatment with blebbistatin at P0, P3 and P5 (Fig. 7F). Interestingly, when PC stiffness increased, there was a concomitant decrease in OHC stiffness (Fig. 7F). Taken together, these data suggest that actin is directly necessary to maintain OHC stiffness and indirectly impacts PC surface mechanical properties early in development.

Outer hair cell and supporting pillar cell stiffness are sensitive to microtubule depolymerization

The increased acetylated tubulin and Young's modulus in PCs between P3 and P5 (Fig. 6) suggested that depolymerizing microtubules could decrease PC stiffness. To test this hypothesis, cochlear cultures were incubated with nocodazole, which prevents microtubule polymerization (Mareel and De Brabander, 1978) and destabilizes microtubules (Lafont et al., 1993). Confocal projections showed decreased β-tubulin I and II immunofluorescence at the lumenal surface of the cochlear epithelium in nocodazole conditions relative to control at P0 (Fig. 8A). Interestingly, the kinocilium, a microtubule-dense structure in OHCs, was unaffected by nocodazole (Fig. 8A, arrowheads) possibly owing to acetylation (Bane et al., 2002; Hammond et al., 2008) and low protein turnover (Zhang et al., 2012).

Next, we determined the effects of disruptions in microtubules on sensory OHC and supporting PC surface mechanical properties. Average Young's modulus was calculated and compared between

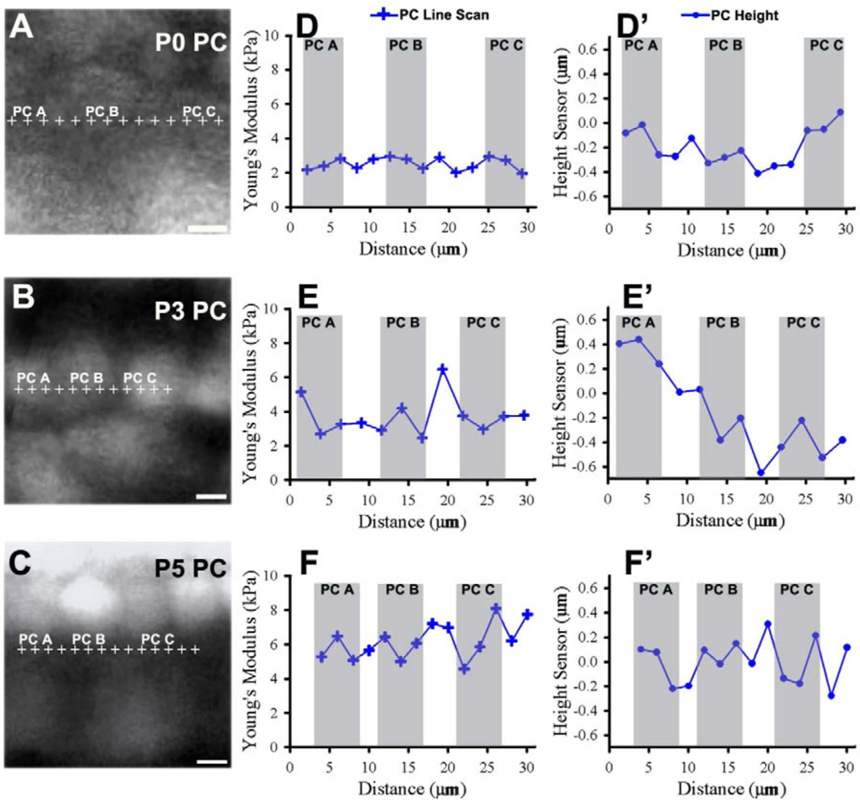

Fig. 5. Supporting pillar cell rows show increasing stiffness but little heterogeneity throughout development. (**A-C**) Fluorescence images of Calcein AM-labeled PCs from P0, P3 and P5 show locations of line scan measurements (+). (**D-F**) PC Young's modulus is plotted across 30 µm longitudinal distance and corresponds to images A-C, respectively. Shaded regions correspond to PCs shown at left. Spaces represent regions that could not be identified as PCs. Data show increasing Young's modulus but little heterogeneity within PC rows from P0 to P5. (**D′-F′**) Relative height (µm) differences in PC row show <0.5 µm variation in shaded regions along the line scan distance (µm). Scale bars: 5 µm.

cultures with nocodazole or vehicle control at P0, P3 and P5. OHC average Young's modulus decreased from 4.13±0.26 kPa to 2.34±0.27 kPa at P0, which showed that microtubule depolymerization significantly softened OHCs at P0 (Fig. 8B; *P*<0.01). However, at P3 and P5, OHC average Young's modulus was not significantly different in nocodazole relative to control conditions (Fig. 8B; *P*>0.10). This suggested that microtubules were dispensable for OHC stiffness at later time points. However, microtubule-dense Deiter's cells (Fig. 6C) were adjacent to OHCs and might have contributed to the stiffness heterogeneity in OHC rows (Fig. 4). To test this hypothesis, AFM line scan measurements were performed on nocodazole-treated cultures and compared with controls at P3, a time when OHC rows exhibit heterogeneity (Fig. 4E), but when OHCs are insensitive to nocodazole treatment (Fig. 8B). We observed that Young's modulus in regions corresponding to OHCs was similar in control and nocodazole conditions (supplementary material Fig. S2, shaded). However, the stiffness heterogeneity was lost in the areas between OHCs (supplementary material Fig. S2, unshaded), which suggests that microtubules contribute to the mechanical properties in OHC rows.

We also examined supporting PC stiffness and found that PC Young's modulus was not significantly different with nocodazole treatment at P0 (Fig. 8B; *P*>0.10). However, there was an increasing disparity in PC stiffness between treatment and control at later time points (Fig. 8B). By P5, PCs were significantly softer with nocodazole (4.9±0.6 kPa) compared with control conditions (10.0±0.8 kPa; *P*<0.01). To look at the stability of microtubules, cultures were also treated with taxol, which binds to β-tubulin (Lowe et al., 2001) and can alter microtbule dynamics (Downing, 2000; Orr et al., 2003). Average Young's modulus of treated OHCs was not significantly different from control at P0, P3 and P5 (Fig. 8C). However, PC surface mechanical properties showed an increasing sensitivity to taxol treatment, with a 58% decrease in stiffness at P3 and a 70% decrease at P5 relative to control (Fig. 8C). Thus, the data suggest that microtubules are necessary for OHC surface mechanical properties early in development and are necessary for PC surface mechanical properties later in development.

The fibroblast growth factor signaling pathway modulates time course of developing cell surface mechanical properties

To begin to explore signaling pathways that could mediate organization of cytoskeletal structures and control developing cell surface mechanical properties, we considered proteins that are active between the late embryonic to early postnatal period. *Fgfr3* is expressed in the developing cochlear sensory epithelium from E16 to P0 (Pickles, 2001; Mueller et al., 2002), has a differential expression pattern in hair cells and supporting cells (Jacques et al., 2007), and plays a role in cochlear morphogenesis (Colvin et al., 1996; Hayashi et al., 2007; Puligilla et al., 2007), making it a potential mediator of cytoskeleton development. To determine the effects of Fgf signaling on the cytoskeleton, cochleae were treated with either Fgf2, which has been shown to bind and activate Fgf receptors, or SU5402, which blocks all Fgf receptors (Mohammadi et al., 1997). An antibody raised to p75 neurotrophin receptor ($p75^{ntr}$) was used to identify differentiated PCs, and previous studies have shown a high correlation between increased $p75^{ntr}$ expression and decreased actin-mediated cell growth (Gestwa et al., 1999; Deponti et al., 2009). Confocal images at P0 and P3 showed increased $p75^{ntr}$ immunofluorescence in supporting cells and decreased phalloidin intensity with Fgf2 treatment, but decreased $p75^{ntr}$ immunofluorescence and increased phalloidin intensity with SU5402 treatment (Fig. 9A). Measuring the relative immunofluorescence revealed a decrease in phalloidin intensity in Fgf2-treated OHCs and PCs and an increase in SU5402-treated OHCs and PCs (Fig. 9B). To examine the effects of Fgf signaling

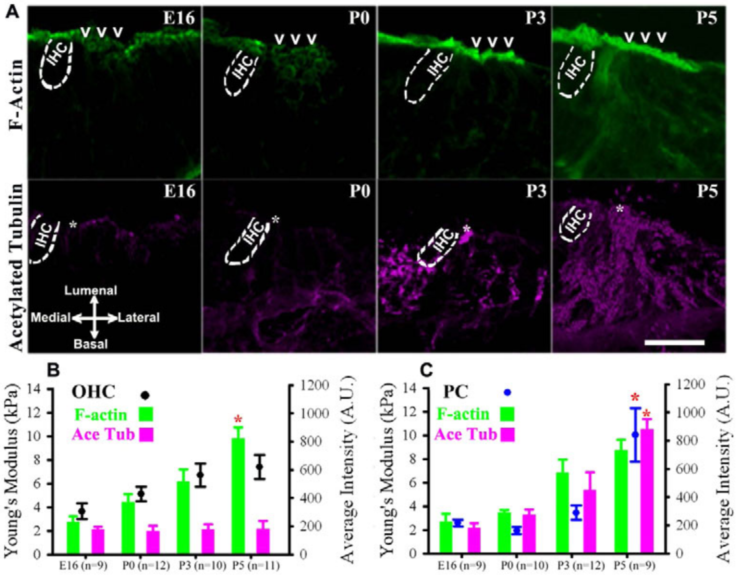
A
E16
P0
P3
P5
F-Actin
Acetylated Tubulin
IHC
Lumenal
Medial
Lateral
Basal
B
OHC
F-actin
Ace Tub
Young's Modulus (kPa)
Average Intensity (A.U.)
E16 (n=9)
P0 (n=12)
P3 (n=10)
P5 (n=11)
C
PC
E16 (n=9)
P0 (n=10)
P3 (n=12)
P5 (n=9)

Fig. 6. Developing OHC and PC surface mechanical properties correspond to acquisition of actin filaments and acetylated microtubules, respectively. (**A**) Representative confocal projections of cochlear cross-sections show gradual increases in F-actin (green) in OHCs (chevrons) from E16 to P5, but abrupt increases in acetylated microtubules (pink) of PCs (asterisks) from P3 to P5. (**B**) Average fluorescence intensity and average Young's modulus (mean±s.e.m.) show gradual increases in OHC stiffness and F-actin immunofluorescence from E16 to P5, whereas acetylated tubulin has relatively consistent intensity. (**C**) A significant increase in PC stiffness from P3 to P5 (*$P<0.01$) was accompanied by a significant increase in acetylated tubulin. Confocal *z*-projections (12 μm) represent apical regions. Scale bar: 10 μm.

on cell surface mechanical properties, average Young's modulus was calculated and compared between cultures treated with either Fgf2 or SU5402 relative to controls. OHCs treated with Fgf2 were >39% softer at P0 and P3 (Fig. 9C; $P<0.01$). However, by P5, OHC average Young's modulus was not significantly different between Fgf2 (8.92±2.38 kPa) and vehicle control (5.59±2.36 kPa) (Fig. 9C). In addition, PC Young's modulus was significantly decreased at P3 in Fgf2-treated explants (3.17±0.54 kPa) relative to control (5.55±1.08 kPa) (Fig. 9C; $P<0.05$). In contrast to Fgf2 treatment, SU5402-treated OHCs and PCs were stiffer at P3 (9.88±0.87 kPa and 9.60±2.47 kPa) and P5 (8.25±0.99 kPa and 27.70±6.48 kPa) compared with untreated OHCs and PCs at P3 (6.75±0.89 kPa and 5.97±1.14 kPa) and P5 (5.51±2.15 kPa and 4.21±0.67 kPa) as measured in the cochlear base (Fig. 9C).

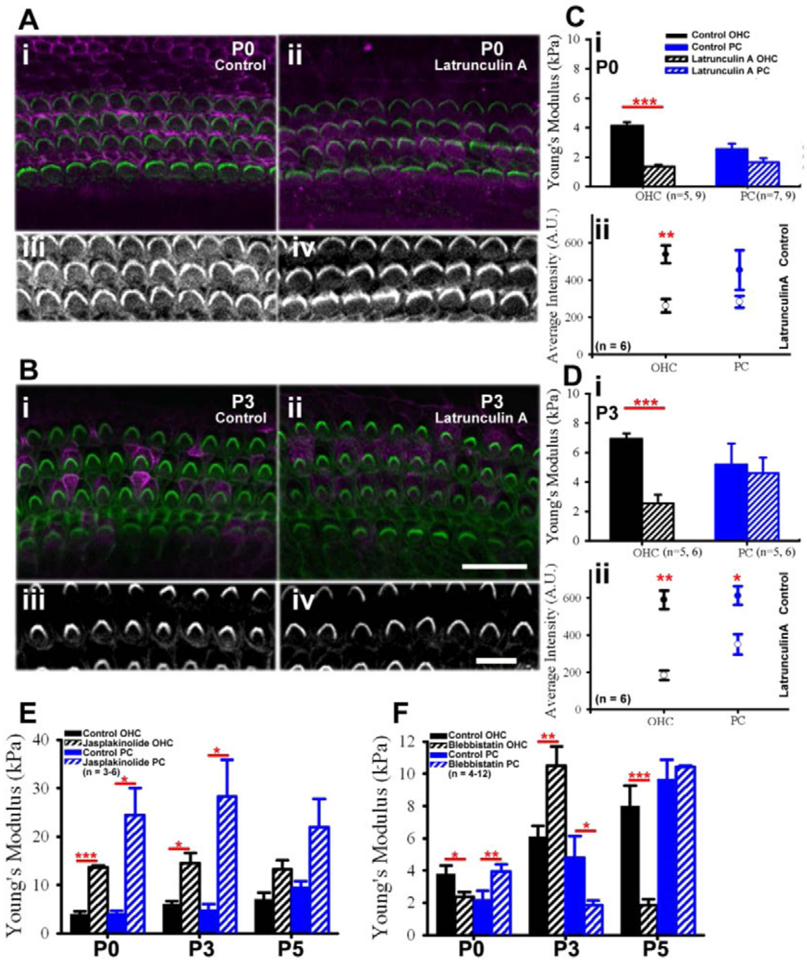
A
i
P0 Control
ii
P0 Latrunculin A
iii
iv
B
P3 Control
P3 Latrunculin A
C
Control OHC
Control PC
Latrunculin A OHC
Latrunculin A PC
Young's Modulus (kPa)
OHC (n=5, 9)
PC (n=7, 9)
Average Intensity (A.U.)
(n = 6)
OHC
PC
LatrunculinA Control
D
P3
OHC (n=5, 6)
PC (n=5, 6)
E
Control OHC
Jasplakinolide OHC
Control PC
Jasplakinolide PC
(n = 3-6)
P0
P3
P5
F
Control OHC
Blebbistatin OHC
Control PC
Blebbistatin PC
(n = 4-12)

Fig. 7. OHC mechanical properties rely primarily on actin. (**A**,**B**) Representative confocal *z*-projections of cochlear explant cultures at P0 and P3 treated with latrunculin A show decreased phalloidin (green) and alterations in distribution of ZO-1 (pink) relative to control. Aiii-iv and Biii-iv show magnified views of *z*-projections highlighting the decrease in phalloidin immunofluorescence (white) in latrunculin A-treated OHCs relative to control conditions at P0 and P3. (**Ci**,**Di**) Young's modulus of OHCs (black) is significantly decreased by latrunculin A at P0 and P3 (***$P<0.001$), but PC (blue) surface mechanical properties are not significantly different. (**Cii**,**Dii**) Fluorescence intensity (mean±s.e.m.) of phalloidin is significantly decreased in latrunculin A-treated OHCs at P0 and P3 and in treated PCs at P3 relative to control (**$P<0.01$, *$P<0.05$). (**E**) Jasplakinolide treatment leads to significant increases in OHC and PC stiffness at P0 and P3. (**F**) Treatment with blebbistatin at P0 leads to a significant decrease in OHC stiffness and significant increase in stiffness of PCs. Treatment at P3 significantly stiffens OHCs, but significantly softens PCs. By P5, blebbistatin-treated OHC stiffness is significantly decreased whereas PC stiffness is not significantly different relative to control condition. Scale bars: in Bii, 20 μm for Ai-ii,Bi-ii; in Biv, 10 μm for Aiii-iv,Biii-iv.

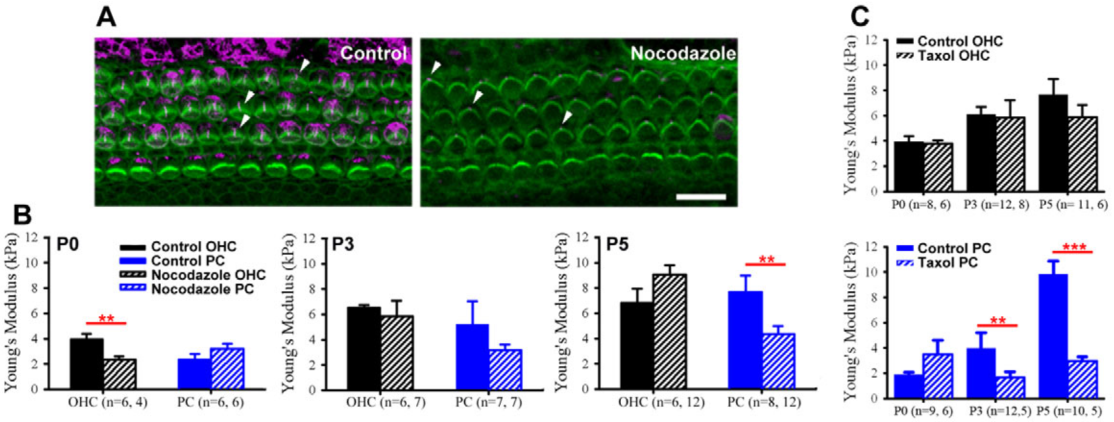

Fig. 8. PC stiffness relies on microtubules. (**A**) Representative confocal *z*-projections of P0 cochlear explant cultures show a decrease in β-tubulin I and II (pink) with nocodazole treatment relative to control. The kinocilium, a microtubule dense structure remains intact (arrowheads). (**B**) Young's modulus (mean±s.e.m.) is significantly decreased in treated OHCs (black) at P0 (**$P<0.01$) but not P3 and P5 ($P>0.10$) and in treated PCs (blue) at P5 but not P0 or P3. (**C**) Average Young's modulus is significantly decreased in taxol-treated PCs at P3 and P5 (***$P<0.001$) but not in OHCs. Scale bar: 10 μm.

Treatment with Fgf2 significantly affected the surface mechanical properties of OHCs and PCs, but on different time scales, suggesting that this signaling pathway might be working through cell-specific downstream signaling cascades. To begin to explore downstream mediators of Fgf signaling, cochleae were cultured in the presence of Fgf2 and one of the following inhibitors: Y27632, which inhibits Rho-associated coiled coil-forming protein serine/threonine kinase (ROCK) and mediates signaling pathways to remodel the actin cytoskeleton (Maekawa et al., 1999; Davies et al., 2000); U0126, which prevents activation of the MAPK kinases MEK-1 and MEK-2 (Favata et al., 1998); and SP600125, which inhibits the Jun N-terminal kinase (JNK) MAPK cascade (Bennett et al., 2001). Average Young's modulus of OHCs was only significantly increased in Fgf2+Y27632-treated cultures at P0 and P3 (Fig. 9D; 6.42±2.69 kPa and 7.57±0.46 kPa, respectively). By contrast, PC average Young's modulus was not only significantly increased in Fgf2+Y27632-treated cultures at P0, but also increased when treated at P3 in combination with Y27632, SP600125 or U0126. It is worth noting that although treatment with inhibitor alone did not significantly impact cell stiffness (data not shown), treatment with SP600125 and U0126 when combined with Fgf2 increased average Young's modulus above control conditions (Fig. 9D; 7.72±2.25 kPa and 7.42±3.21 kPa, respectively), which further supports the additional non-specific effects of these inhibitors (Davies et al., 2000). In summary, downregulation of Fgfrs had an effect on actin distribution and increased both OHC and PC stiffness. By contrast, upregulation of Fgf signaling had an effect on actin that could be rescued by the compensatory effects of Y27632 on the actin cytoskeleton of both OHCs and PCs.

DISCUSSION

In this paper, we investigated the relationship between cytoskeleton development and changing cell surface mechanical properties in the maturing inner ear. Results suggest that OHC surface mechanical properties increase with the developing actin network and have a decreasing dependence on microtubules, whereas PC stiffness has an increasing dependence on microtubules. In addition, these data suggest that cytoskeletal structures mediate developing OHC and PC surface mechanical properties, and that cell stiffness can be affected by signaling cascades, such as the Fgf pathway, through changes in cytoskeleton dynamics (Fig. 10), which might contribute to the morphogenesis of this sensory epithelium during postnatal development.

Cytoskeletal architecture mediates developing mechanical properties

Sensory OHCs and non-sensory PCs have distinct morphologies specified, in part, by cytoskeletal structures (Anniko, 1983). Our data indicate that OHCs develop mechanical properties that are distinct from PCs (Fig. 3), which might reflect the sensory and supporting roles of these cell types in development. Although we directly probed the actin-rich cuticular plate at the OHC lumenal surface, we were unable to explore the basolateral actin content previously described in dissociated OHCs (Tolomeo and Holley, 1997; Murakoshi et al., 2006), which contributes to the heterogeneity in OHC Young's modulus between apical and basolateral areas at adult stages (Zelenskaya et al., 2005; Murakoshi et al., 2006). Instead, by making measurements within the semi-intact organ of Corti, we were able to describe cell-specific changes in surface mechanical properties of this tissue along OHC rows and not PC rows (Figs 4, 5), which might inform future theoretical models of cochlear morphogenesis. These data also suggest that cell stiffness increases in areas near cell boundaries (Fig. 4) are probably due to supporting Deiter's cell projections that interdigitate between OHCs (Anniko, 1983). With future experiments, it might be possible to examine the indirect impact of these junctions on OHC surface mechanical properties.

To understand the time course of developing PC stiffness, we studied cytoskeletal architecture with electron microscopy and immunofluorescence imaging. We found that the increased microtubule density in PCs between P0 and P5 (Fig. 2) was not sufficient to explain the abrupt PC stiffening between P3 and P5 (Fig. 6). Instead, we find that this increase in stiffness coincides more with the increase in acetylated microtubules (Fig. 6). Previous results have observed increases in microtubule stability upon acetylation (Bane et al., 2002; Hammond et al., 2008). Therefore, these results further the argument that post-translational modifications of microtubules might impart the stability necessary for maturing PC mechanical properties (Tolomeo and Holley, 1997). Using these measurements, future studies will explore how cytoskeletal dynamics are regulated in PCs to both exert and resist mechanical stresses of postnatal cochlear development.

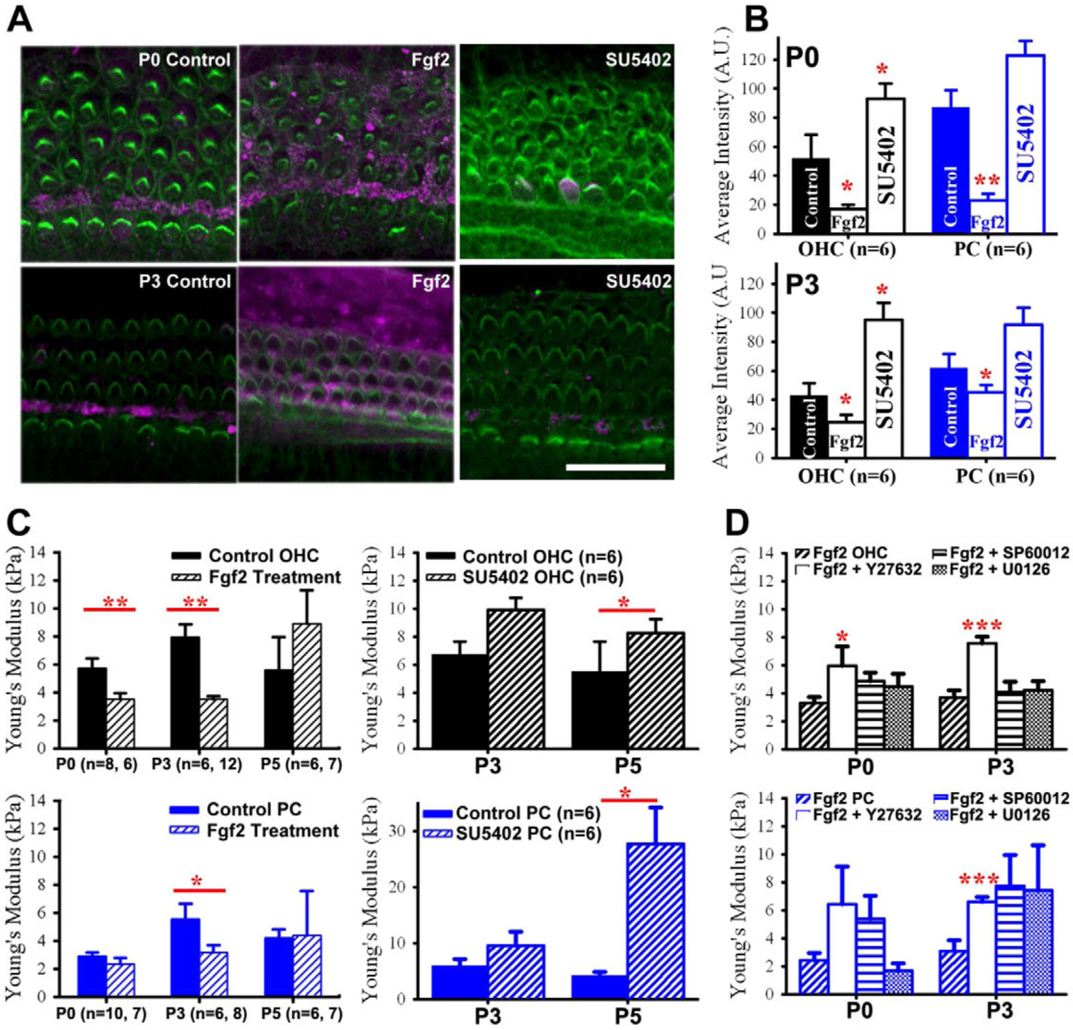

Fig. 9. Fgf signaling pathway modulates time course of developing cell mechanical properties. (**A**) Representative confocal *z*-projections at P0 and P3 show an increase in p75^{ntr} (pink) in PCs and DCs, and a decrease in phalloidin (green) in OHCs after Fgf2 treatment. Treatment with SU5402 at P0 and P3 show decreases in p75^{ntr} immunofluorescence in PCs and increases in phalloidin in OHCs. (**B**) Relative phalloidin immunofluorescence (mean±s.e.m.) shows decreased intensity in Fgf2-treated OHCs and PCs, and increased intensity in SU5402-treated OHCs and PCs relative to control conditions. (**C**) Young's modulus (mean±s.e.m.) is significantly decreased in Fgf2-treated OHCs at P0 and P3, and in PCs at P3 relative to control. Average Young's modulus is significantly increased in SU5402-treated OHCs and PCs at P5 relative to control. (**D**) Average Young's modulus from six to nine cultures shows that the softening of OHCs and PCs in response to Fgf2 is compensated only when treated in combination with ROCK inhibitor Y27632. $^*P<0.05$, $^{**}P<0.01$, $^{***}P<0.001$. Scale bar: 20 μm.

Cell surface mechanical properties might mediate ongoing cochlear morphogenesis

Our finding that OHCs and PCs stiffen in response to jasplakinolide is not unexpected, given that actin is present in both cell types and that this drug is known to polymerize actin (Bubb et al., 2000), supporting our finding that increases in actin filaments during development might be responsible for increasing cell stiffness. However, the finding that only OHC stiffness is decreased in the presence of latrunculin A (Fig. 7) suggests a crucial need for actin to develop OHC surface mechanical properties. Furthermore, these surface mechanical properties describe a subset of the cytoskeleton that has previously been shown to be essential for the organization of the actin-based cuticular plate (Sobkowicz et al., 1995; Nishida et al., 1998), which contributes to formation of the stereocilia bundle (Furness et al., 2005; Perrin et al., 2010; Etournay et al., 2010). However, the finding that OHCs soften after treatment with nocodazole also implicates microtubules in cuticular plate formation. This is consistent with experiments showing that early postnatal OHCs recover from mechanical damage by first reforming a microtubule-based kinocilium and then re-growing stereocilia (Sobkowicz et al., 1995). Therefore, the transient role for microtubules in OHC stiffness might act as a foundation for organization of the actin-based cuticular plate and, in part, for the organization of stereocilia.

Surrounding these sensory hair cells are many types of non-sensory supporting cells, which are thought to have either metabolic (Wangemann and Liu, 1996; Kikuchi et al., 2000) or structural (Tolomeo and Holley, 1997; Mogensen et al., 1998) roles in hearing. To explore the structural role of pillar cells, we investigated the impact of both actin filaments and microtubules. Our finding that PC Young's modulus is not significantly affected by latrunculin A treatment suggests that actin alone is not sufficient to develop PC surface mechanical properties. In contrast to the OHCs, PC stiffness was most sensitive to microtubule disruptions

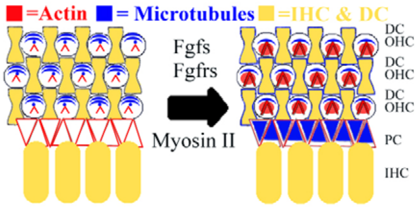

Fig. 10. Developing cell stiffness is dependent on cytoskeletal structure in the organ of Corti. Taken together, results reported here suggest that from late embryonic (left) to early postnatal (right) development, outer hair cells (OHCs) have an increasing reliance on the actin network (red) and a decreasing reliance on microtubules (blue). By contrast, supporting pillar cells (PCs) rely partly on actin early in development, and have an increasing reliance on microtubules. Furthermore, fibroblast growth factors (Fgfs), fibroblast growth factor receptors (Fgfrs) and myosin II contribute to the time course of developing cell mechanical properties. IHC, inner hair cell; DC, Deiter's cell.

(Fig. 8), which have the potential to alter the PC resistance to applied forces during tissue development. However, microtubules are probably interconnected to some extent with the actin cytoskeleton, as supported by the intriguing finding that OHCs and PCs show opposite changes in response to blebbistatin treatment at similar time points (Fig. 7). This might be due in part to different distributions of myosin II (Yamamoto et al., 2009) driving the dynamic organization of PCs and OHCs and generating forces on actin filaments (Bertet et al., 2004; Cai et al., 2010). Our results suggest that both microtubules and myosin II mediate the ongoing mechanical development of this tissue and, therefore, might contribute to the formation of the tunnel of Corti, a fluid-filled structure that rests between inner and outer hair cells that is necessary for proper hearing (Li et al., 1999; Puligilla et al., 2007; Minekawa et al., 2009). With this work, future studies can build on these measurements to include molecular mediators that work to coordinate cytoskeletal dynamics to form fluid-filled spaces within the postnatal organ of Corti.

Molecular pathways that control cell stiffness might mediate therapeutic intervention of damaged epithelia

To begin to identify signaling pathways that could mediate developing cell structure and mechanical properties, we modulated Fgf signaling. This pathway has been known to regulate cell differentiation, cell migration and cell shape (Ornitz, 2000). By investigating the effect of Fgf on the cytoskeleton, we find that treatment with Fgf2 softens OHCs and PCs, supporting previous reports that activation of Fgf signaling prevents cellular differentiation in the organ of Corti (Mueller et al., 2002; Jacques et al., 2007). By contrast, inhibition of Fgf receptor activity stiffens OHCs and PCs, suggesting that there might be a premature maturation of some aspects of both cell types. Taken together, these data implicate another role for Fgf signaling, in cell mechanical properties, through changes in actin dynamics.

Finally, the effects of Fgf signaling on cell surface mechanical properties (Fig. 9) outline a critical period in early postnatal development for this pathway to alter the cytoskeleton. By examining downstream inhibitors of this signaling cascade, we provide insights that link this pathway to actin dynamics via ROCK, which might account, at least in part, for the observed rescue of cell stiffness. Furthermore, recent work in the developing vestibular epithelium has suggested a possible role for increased actin in the inhibition of hair cell regeneration (Burns et al., 2008). Results presented here suggest that treatment with Fgfs, which act to prevent actin polymerization in hair cells, could be considered as a potential intervention in actin-belt formation in supporting cells, and as a key component to consider when trying to repair damaged epithelia.

Acknowledgements

We thank Ya-Xian Wang for help with tissue preparation for TEM, and T. B. Friedman and Anders Fridberger for comments on an earlier version of this manuscript.

Funding

This research was supported by the National Institute on Deafness and other Communication Disorders (NIDCD) Intramural Research Program [DC000059 to M.W.K., DC000033 to R.S.C.] and in part with an Intramural Fellowship to Promote Diversity from the National Institutes of Health Office of the Director [K.B.S.]. Deposited in PMC for release after 12 months.

Competing interests statement

The authors declare no competing financial interests.

Supplementary material

Supplementary material available online at
http://dev.biologists.org/lookup/suppl/doi:10.1242/dev.073734/-/DC1

References

Anniko, M. (1983). Cytodifferentiation of cochlear hair cells. *Am. J. Otolaryngol.* **4**, 375-388.

Ayscough, K. R., Stryker, J., Pokala, N., Sanders, M., Crews, P. and Drubin, D. G. (1997). High rates of actin filament turnover in budding yeast and roles for actin in establishment and maintenance of cell polarity revealed using actin inhibitor latrunculin-A. *J. Cell Biol.* **137**, 399-416.

Bane, B. C., MacRae, T. H., Xiang, H., Bateman, J. and Slepecky, N. B. (2002). Microtubule cold stability in supporting cells of the gerbil auditory sensory epithelium: correlation with tubulin post-translational modifications. *Cell Tissue Res.* **307**, 57-67.

Bennett, B. L., Sasaki, D. T., Murray, B. W., O'Leary, E. C., Sakata, S. T., Xu, W., Leisten, J. C., Motiwala, A., Pierce, S., Satoh, Y. et al. (2001). SP600125, an anthrapyrazolone inhibitor of Jun N-terminal kinase. *Proc. Natl. Acad. Sci. USA* **98**, 13681-13686.

Bershadsky, A. D., Glück, U., Denisenko, O. N., Sklyarova, T. V., Spector, I. and Ben-Ze'ev, A. (1995). The state of actin assembly regulates actin and vinculin expression by a feedback loop. *J. Cell Sci.* **108**, 1183-1193.

Bertet, C., Sulak, L. and Lecuit, T. (2004). Myosin-dependent junction remodeling controls planar cell intercalation and axis elongation. *Nature* **429**, 667-671.

Bridgman, P. C., Dave, S., Asnes, C. F., Tullio, A. N. and Adelstein, R. S. (2001). Myosin IIB is required for growth cone motility. *J. Neurosci.* **21**, 6159-6169.

Bubb, M. R., Senderowicz, A. M., Sausville, E. A., Duncan, K. L. and Korn, E. D. (1994). Jasplakinolide, a cytotoxic natural product, induces actin polymerization and competitively inhibits the binding of phalloidin to F-actin. *J. Biol. Chem.* **269**, 14869-14871.

Bubb, M. R., Spector, I., Beyer, B. B. and Forsen, K. M. (2000). Effects of jasplakinolide on the kinetics of actin polymerization. An explanation for certain in vivo observations. *J. Biol. Chem.* **275**, 5163-5170.

Burns, J., Christophel, J. J., Collado, M. S., Magnus, C., Carfrae, M. and Corwin, J. T. (2008). Reinforcement of cell junctions correlates with the absence of hair cell regeneration in mammals and its occurrence in birds. *J. Comp. Neurol.* **511**, 396-414.

Cai, Y., Rossier, O., Gauthier, N. C., Biais, N., Fardin, M. A., Zhang, X., Miller, L. W., Ladoux, B., Cornish, V. W. and Sheetz, M. P. (2010). Cytoskeletal coherence requires myosin-IIA contractility. *J. Cell Sci.* **123**, 413-423.

Colvin, J. S., Bohne, B. A., Hardin, G. W., McEwen, D. G. and Ornitz, D. M. (1996). Skeletal overgrowth and deafness in mice lacking fibroblast growth factor receptor 3. *Nat. Genet.* **12**, 390-397.

Coué, M., Brenner, S. L., Spector, I. and Korn, E. D. (1987). Inhibition of actin polymerization by latrunculin A. *FEBS Lett.* **213**, 316-318.

Davies, S. P., Reddy, H., Caivano, M. and Cohen, P. (2000). Specificity and mechanism of action of some commonly used protein kinase inhibitors. *Biochem. J.* **351**, 95-105.

Deponti, D., Buono, R., Catazaro, G., De Palma, C., Longhi, R., Meneveri, R., Bresolin, N., Bassi, M. T., Cossu, G., Clementi, E. et al. (2009). The low-affinity for neurotrophins p75NTR plays a key role for satellite cell function in muscle repair acting via RhoA. *Mol. Biol. Cell* **20**, 3620-3627.

Downing, K. H. (2000). Structural basis for the interaction of tubulin with proteins and drugs that affect microtubule dynamics. *Annu. Rev. Cell Dev. Biol.* **16**, 89-111.

Etournay, R., Lepelletier, L., Boutet de Monvel, J., Michel, V., Cayet, N., Leibovici, M., Weil, D., Foucher, I., Hardelin, J. P. and Petit, C. (2010). Cochlear outer hair cells undergo an apical circumference remodeling constrained by the hair bundle shape. *Development* **137**, 1373-1383.

Favata, M. F., Horiuchi, K. Y., Manos, E. J., Daulerio, A. J., Stradley, D. A., Feeser, W. S., Van Dyk, D. E., Pitts, W. J., Earl, R. A., Hobbs, F. et al. (1998). Identification of a novel inhibitor of mitogen-activated protein kinase kinase. *J. Biol. Chem.* **273**, 18623-18632.

Fritzsch, B., Beisel, K. W., Jones, K., Fariñas, I., Maklad, A., Lee, J. and Reicherdt, L. F. (2002). Development and evolution of inner ear sensory epithelia and their innervation. *J. Neurobiol.* **53**, 143-156.

Furness, D. N., Katori, Y., Mahendrasingam, S. and Hackney, C. M. (2005). Differential distribution of β- and γ-actin in guinea pig cochlear sensory and supporting cells. *Hear. Res.* **207**, 22-34.

Gavara, N. and Chadwick, R. S. (2010). Noncontact microreheology at acoustic frequencies using frequency-modulated atomic force microscopy. *Nat. Methods* **7**, 650-654.

Gestwa, G., Wiechers, B., Zimmerman, U., Praetorius, M., Rohbock, K., Köpschall, I., Zenner, H. P. and Knipper, M. (1999). Differential expression of trkB.T1 and trkB.T2, truncated trkC, and p75 (NGFR) in the cochlea prior to hearing function. *J. Comp. Neurol.* **414**, 33-49.

Guha, M., Zhou, M. and Wang, Y. L. (2005). Cortical actin turnover during cytokinesis requires myosin II. *Curr. Biol.* **15**, 732-736.

Hallworth, R., McCoy, M. and Polan-Curtain, J. (2000). Tubulin expression in the developing and adult gerbil organ of Corti. *Hear. Res.* **139**, 31-41.

Hammond, J., Cai, D. and Verhey, K. J. (2008). Tubulin modifications and their cellular functions. *Curr. Opin. Cell Biol.* **20**, 71-76.

Hayashi, T., Cunningham, D. and Bermingham-McDonogh, O. (2007). Loss of FGFR3 leads to excess hair cell development in the mouse organ of corti. *Dev. Dyn.* **236**, 525-533.

Jacques, B. E., Montocouquiol, M. E., Layman, E. M., Lewandoski, M. and Kelley, M. W. (2007). Fgf8 induces pillar cell fate and regulates cellular patterning in the mammalian cochlea. *Development* **134**, 3021-3029.

Janmey, P. A. (1998). The cytoskeleton and cell signaling: component localization and mechanical coupling. *Phys. Rev.* **78**, 763-781.

Karavitaki, K. D. and Mountain, D. C. (2007). Evidence for outer hair cell driven oscillatory fluid flow in the tunnel of corti. *Biophys. J.* **92**, 3284-3293.

Kelley, M. W. (2007). Cellular commitment and differentiation in the organ of Corti. *Int. J. Dev. Biol.* **51**, 571-583.

Kelly, M. and Chen, P. (2007). Shaping the mammalian auditory sensory organ by the planar cell polarity pathway. *Int. J. Dev. Biol.* **51**, 535-547.

Kikuchi, T., Kimura, R. S., Paul, D. L., Takasaka, T. and Adams, J. C. (2000). Gap junction systems in the mammalian cochlea. *Brain Res. Brain Res. Rev.* **32**, 163-166.

Kovacs, M., Toth, J., Hetenyi, C., Malnasi-Csizmadia, A. and Sellers, J. R. (2004). Mechanism of blebbistatin inhibition of myosin II. *J. Biol. Chem.* **279**, 355557-355563.

Lafont, F., Rouget, M., Rousselet, A., Valenza, C. and Prochiantz, A. (1993). Specific responses of axons and dendrites to cytoskeleton perturbations: an in vitro study. *J. Cell Sci.* **104**, 433-443.

Lane, N. E. and Yao, W. (2010). Glucocorticoid-induced bone fragility. *Ann. N. Y. Acad. Sci.* **1192**, 81-83.

Li, D., Henley, C. M. and O'Malley, B. W., Jr (1999). Distortion product otoacoustic emissions and outer hair cell defects in the hyt/hyt mutant mouse. *Hear. Res.* **138**, 65-72.

Limouze, J., Straight, A. F., Mitchison, T. and Sellers, J. R. (2004). Specificity of blebbistatin, an inhibitor of myosin II. *J. Muscle Res. Cell Motil.* **25**, 337-341.

Lowe, J., Li, H., Downing, K. H. and Nogales, E. (2001). Refined structure of alpha beta-tubulin at 3.5 A resolution. *J. Mol. Biol.* **313**, 1045-1057.

Maekawa, M., Ishizaki, T., Boku, S., Watanabe, N., Fujita, A., Iwamatsu, A., Obinata, T., Ohashi, K., Mizuno, K. and Narumiya, S. (1999). Signaling from Rho to the actin cytoskeleton through protein kinases ROCK and LIM-kinase. *Science* **285**, 895-898.

Mammoto, T. and Ingber, D. E. (2010). Mechanical control of tissue and organ development. *Development* **137**, 1407-1420.

Mareel, M. M. and De Brabander, M. J. (1978). Effect of microtubule inhibitors on malignant invasion in vitro. *J. Natl. Cancer Inst.* **61**, 787-792.

Minekawa, A., Abe, T., Inoshita, A., Iizuka, T., Kakehata, S., Narui, Y., Koike, T., Kamiya, K., Okamura, H. O., Shinkawa, H. et al. (2009). Cochlear outer hair cells in a dominant-negative connexin26 mutant mouse preserve non-linear capacitance in spite of impaired distortion product otoacoustic emission. *Neuroscience* **164**, 1312-1319.

Mogensen, M. M., Henderson, C. G., Mackie, J. B., Lane, E. B., Garrod, D. R. and Tucker, J. B. (1998). Keratin filament deployment and cytoskeletal networking in a sensory epithelium that vibrates during hearing. *Cell Motil. Cytoskeleton* **41**, 138-153.

Mohammadi, M., McMahon, G., Sun, L., Tang, C., Hirth, P., Yeh, B. K., Hubbard, S. R. and Schlessinger, J. (1997). Structures of the tyrosine kinase domain of fibroblast growth factor receptor in complex with inhibitors. *Science* **276**, 955-960.

Montcouquiol, M. and Kelley, M. W. (2003). Planar and vertical signals control cellular differentiation and patterning in the mammalian cochlea. *J. Neurosci.* **23**, 9469-9478.

Mueller, K. L., Jacques, B. E. and Kelley, M. W. (2002). Fibroblast growth factor signaling regulates pillar cell development in the organ of corti. *J. Neurosci.* **22**, 9368-9377.

Murakoshi, M., Yoshida, N., Iida, K., Kumano, S., Kobayashi, T. and Wada, H. (2006). Local mechanical properties of mouse outer hair cells: atomic force microscopy study. *Auris Nasus Larynx* **33**, 149-157.

Murthy, K. and Wadsworth, P. (2005). Myosin-II-dependent localization and dynamics of F-actin during cytokinesis. *Curr. Biol.* **15**, 724-731.

Naidu, R. C. and Mountain, D. C. (1998). Measurements of the stiffness map challenge a basic tenet of cochlear theories. *Hear. Res.* **124**, 124-131.

Nishida, Y., Rivolta, M. N. and Holley, M. C. (1998). Timed markers for the differentiation of the cuticular plate and stereocilia in hair cells from the mouse inner ear. *J. Comp. Neurol.* **395**, 18-28.

Ornitz, D. M. (2000). FGFs, heparin sulfate, and FGFRs: complex interactions essential for development. *Bioessays* **22**, 108-112.

Orr, G. A., Verdier-Pinard, P., McDaid, H. and Horwitz, S. B. (2003). Mechanisms of Taxol resistance related to microtubules. *Oncogene* **22**, 280-295.

Perrin, B. J., Sonnemann, K. J. and Ervasti, J. M. (2010). β-actin and γ-actin are each dispensible for auditory hair cell development but required for stereocilia maintenance. *PLoS Genet.* **6**, e1001158.

Petralia, R. S. and Wenthold, R. J. (1992). Light and electron immunocytochemical localization of AMPA-selective glutamate receptors in the rat brain. *J. Comp. Neurol.* **318**, 329-354.

Pickles, J. O. (2001). The expression of fibroblast growth factors and their receptors in the embryonic and neonatal mouse inner ear. *Hear. Res.* **155**, 54-62.

Pujol, R. and Hilding, D. (1973). Anatomy and physiology of the onset of auditory function. *Acta Otolaryngol.* **76**, 1-10.

Puligilla, C., Feng, F., Ishikawa, K., Bertuzzi, S., Dabdoub, A., Griffith, A. J., Fritzsch, B. and Kelley, M. W. (2007). Disruption of fibroblast growth factor receptor 3 signaling results in defects in cellular differentiation, neuronal patterning and hearing impairment. *Dev. Dyn.* **236**, 1905-1917.

Raphael, Y., Athey, B. D., Wang, Y., Lee, M. K. and Altschuler, R. A. (1994). F-actin and spectrin in the organ of corti: comparative distribution in different cell types and mammalian species. *Hear. Res.* **76**, 173-187.

Rasband, W. S. (1997). ImageJ, U.S. National Institutes of Health, Bethesda, Maryland, USA, http://rsb.info.nih.gov/ij.

Safar, M. E., London, G. M. and Plante, G. E. (2004). Arterial stiffness and kidney function. *Hypertension* **43**, 163-168.

Scherer, M. P. and Gummer, A. W. (2004). Impedance analysis of the organ of corti with magnetically actuated probes. *Biophys. J.* **87**, 1378-1391.

Self, T., Sobe, T., Copeland, N. G., Jenkins, N. A., Avraham, K. B. and Steel, K. P. (1999). Role of myosin VI in the differentiation of cochlear hair cells. *Dev. Biol.* **214**, 331-341.

Slepecky, N. and Chamberlain, S. C. (1985). Immunoelectron microscopic and immunofluorescent localization of cytoskeletal and muscle-like contractile proteins in inner ear sensory hair cells. *Hear. Res.* **20**, 245-260.

Sneddon, I. N. (1965). The relation between load and penetration in the axisymmetric Boussinesq problem for a punch of arbitrary profile. *Int. J. Eng. Sci.* **3**, 47-57.

Sobkowicz, H. M., Slapnick, S. M. and August, B. K. (1995). The kinocilium of auditory hair cells and evidence for its morphogenetic role during the regeneration of stereocilia and cuticular plates *J. Neurocyt.* **24**, 633-653.

Straight, A. F., Cheung, A., Limouze, J., Chen, I., Westwood, N. J., Sellers, J. R. and Mitchison, T. J. (2003). Dissecting temporal and spatial control of cytokinesis with a myosin II Inhibitor. *Science* **299**, 1743-1747.

Tolomeo, J. A. and Holley, M. C. (1997). Mechanics of microtubule bundles in pillar cells from the inner ear. *Biophys. J.* **73**, 2241-2247.

Tolomeo, J. A., Steele, C. R. and Holley, M. C. (1996). Mechanical properties of the lateral cortex of mammalian auditory outer hair cells. *Biophys. J.* **71**, 421-429.

Wangemann, P. and Liu, J. (1996). Osmotic water permeability of capillaries from the isolated spiral ligament: new in-vitro techniques for the study of vascular permeability and diameter. *Hear. Res.* **95**, 49-56.

Westermann, S. and Weber, K. (2003). Post-translational modifications regulate microtubule function. *Nat. Rev. Mol. Cell Biol.* **4**, 938-947.

Yamamoto, N., Okano, T., Ma, X., Adelstain, R. S. and Kelley, M. W. (2009). Myosin II regulates extension, growth and patterning in the mammalian cochlear duct. *Development* **136**, 1977-1986.

Zelenskaya, A., Boutet de Monvel, J., Pesen, D., Radmacher, M., Hoh, J. H. and Ulfendahl, M. (2005). Evidence for highly elastic shell-core organization of cochlear outer hair cells by local membrane indentation. *Biophys. J.* **88**, 2982-2993.

Zhang, D. S., Piazza, V., Perrin, B. J., Rzadzinska, A. K., Poczatek, J. C., Wang, M., Prosser, H. M., Ervasti, J. M., Corey, D. P. and Lechene, C. P. (2012). Multi-isotope imaging mass spectrometry reveals slow protein turnover in hair-cell stereocilia. *Nature* **481**, 520-524.